

A New Dispersion Entropy and Fuzzy Logic System Methodology for Automated Classification of Dementia Stages using Electroencephalograms

Juan P. Amezcua-Sanchez¹, Nadia Mammone², Francesco C. Morabito², and Hojjat Adeli^{4,*}

¹ Autonomous University of Queretaro (UAQ), Faculty of Engineering, Departments Biomedical and Electromechanical, Campus San Juan del Río, Río Moctezuma 249, Col. San Cayetano, C. P. 76807, San Juan del Río, Qro., México.

² Department DICEAM of the Mediterranean University of Reggio Calabria, 89060 Reggio Calabria, Italy.

⁴ Departments of Biomedical Informatics and Neuroscience, The Ohio State University, 470 Hitchcock Hall, 2070 Neil Avenue, Columbus, OH 43220 U.S.A.

*Corresponding author: adeli.1@osu.edu

ABSTRACT

A new EEG-based methodology is presented for differential diagnosis of the Alzheimer's disease (AD), Mild Cognitive Impairment (MCI), and healthy subjects employing the discrete wavelet transform (DWT), dispersion entropy index (DEI), a recently-proposed nonlinear measurement, and a fuzzy logic-based classification algorithm. The effectiveness and usefulness of the proposed methodology are evaluated by employing a database of measured EEG data acquired from 135 subjects, 45 MCI, 45 AD and 45 healthy subjects. The proposed methodology differentiates MCI and AD patients from HC subjects with an accuracy of 82.6-86.9%, sensitivity of 91%, and specificity of 87%.

Keywords: Mild Cognitive Impairment, Alzheimer's disease, Discrete wavelet transform, Fuzzy logic, Electroencephalograms.

1. INTRODUCTION

Alzheimer's disease (AD) is known as the most common neurological disorder after stroke and the most common form of neurodegenerative dementia in elderly, which causes a progressive loss of diverse cognitive abilities such as memory, reasoning, among others (Blennow et al. 2006; Vuksanovic et al. 2019; Collazos-Huertas et al. 2019). Mild cognitive impairment (MCI), an initial or prodromal stage of AD, produces a slight decline in mental

abilities of people, which allows maintaining their autonomy and ordinary life (Petersen et al. 2001, Gauthier et al. 2006; Carrillo et al. 2018). Annually, 10-15% of MCI patients progress to dementia (Mitchell and Shiri-Feshki, 2009). For this reason, developing approaches or methodologies for automated diagnosis of the onset of cognitive disease accurately is of paramount importance so that patients can be enrolled in appropriate clinical treatments with the goal of delaying the effects of the disease and reducing the conversion from MCI to AD.

In the last twenty years, the electroencephalography (EEG) (Zhang et al. 2019; Ibáñez-Molina et al. 2019) and magnetoencephalography (MEG) (Corsi et al. 2019; Martinez-Vargas et al. 2019) have demonstrated to be promising tools for finding non-invasive markers for assisting in the automated diagnostic of patients with MCI or AD (Fang et al., 2018; Nobukawa et al. 2019), and other neurological diseases such as Parkinson (Gálvez et al., 2018), epilepsy (Shanir et al. 2017; Acharya et al. 2018; Sun et al. 2019; Ansari et al. 2019), autism spectrum disorder (Ibrahim et al., 2018; Luttia et al., 2019), major depressive disorder (Mumtaz et al., 2018), sleep disorder (Zieleniewska et al. 2019), and for driver fatigue detection (Cail et al. 2019), person identification (Schetinin et al. 2018) among other disorders.

MCI and AD produce minute changes in the measured EEG and MEG signals compared with the signals measured in healthy subjects, which can be invisible even to trained clinical neurophysiologists, especially for MCI patients, representing a research challenge for the identification of patterns or features capable of distinguishing between a healthy person and a person with MCI or AD. Hence, an effective signal processing and pattern recognition technique capable of discovering and estimating appropriate patterns or features in patients with MCI or AD is highly desirable. **Authors' research hypothesis is** that only a multi-paradigm approach through integration or combination of various computing and information processing paradigms can solve such a complicated time-series pattern recognition problem effectively and accurately (Adeli et al. 2005a&b; Hulbert and Adeli 2013; Bhat et al. 2015; Mirzaei et al. 2016; deEtoile and Adeli, 2017). In this regard, recent methods have been introduced in the literature for automated diagnosis of AD and MCI using EEG or MEG. For example, Trambaiolli et al. (2011) combined the coherence method and spectral peak (the point in EEG power spectral density (PSD) where spectral energy reaches

its maximum value) estimated by Fourier transform along with a support vector machine (Zhang et al. 2019) for diagnosis of patients with AD. The authors reported an accuracy of 79.9% discerning normal subjects and patients with AD. Entropy analysis has been used in many EEG studies (Martínez-Rodrigo et al. 2019). Bruña et al. (2012) used the Shannon entropy method for discriminating normal subjects from MCI patients using MEG signals. They reached an accuracy of 65% by using the variation in the entropy value of MCI patients compared with normal subjects at the frontal area of brain. Ahmadlou et al. (2014) introduced two new nonlinear measurements named graph efficiency complexity and index complexity for diagnosis of MCI patients using the MEG signals acquired during a Sternberg task. They noted that the graph efficiency complexity method allows differentiating MCI and normal patients with a high accuracy of 97.6%. Houmani et al. (2015) compared the Shannon entropy, the correlation dimension, and the epoch-based entropy (EE) for diagnosis of AD. They found that EE is more effective than Shannon entropy and correlation dimension for distinguishing AD from normal subjects, reaching an accuracy of 83%. Following the multi-paradigm approach mentioned earlier, Amezquita-Sanchez et al. (2016) presented a new methodology for classification of normal and MCI patients based on the integration of the complete ensemble empirical mode decomposition, permutation entropy, and the enhanced probabilistic (EPNN) of Ahmadou and Adeli (2010), achieving a high accuracy of 98.4%. Timothy et al. (2017) employed the combined recurrence and cross recurrence quantification analysis for the diagnosis of MCI during a short-term memory task and resting eyes closed, reaching an accuracy of 70%. Triggiani et al (2017) employed a backpropagation neural network for distinguishing between normal subjects and AD patients during resting eyes closed, using EEG signals, achieving an accuracy of 77%. Simons et al. (2018) compared the fuzzy entropy (FE), the sample entropy (SE), and approximate entropy (AE) for diagnosis of AD using EEG signals. The authors mention that FE is more effective than SE and AE for distinguishing AD from normal subjects when the patterns obtained by FE methods is combined with a support vector machine (SVM) classifier, reaching an accuracy of 86.3%.

The previous methodologies have reported promising results for diagnosis of a single disease, AD or MCI. A few researchers have attempted to develop methodologies capable of classifying or distinguishing different dementia stages, MCI, and AD patients (Morabito et al. 2016). These efforts are all based on EEGs. Mammone et al. (2017) introduced a nonlinear

measurement, named permutation disalignment index (PDI), for differential diagnosis of MCI and AD patients employing EEG recordings. They observed an increase of the PDI value in two frequency bands, delta and theta, of patients with MCI converted to AD. Houmani et al. (2018) combined two nonlinear measurements named epoch-based entropy and bump modeling with an SVM for distinguishing AD, MCI and subjective cognitive impairment patients using the EEG signals acquired during an eye-closed resting state, reaching an accuracy of 81%. Recently, Amezcua-Sanchez et al. (2019) presented a novel EEG-based methodology based on integration of multiple signal classification, empirical wavelet transform, nonlinear indices, fractal dimension and Hurst exponent, and EPNN for distinguishing MCI and AD patients. The authors reported that the proposed method allows differentiating between MCI and AD patients with a high accuracy of 90.3%, but noted that an additional investigation with a larger database is required to confirm the preliminary results. Ieracitano et al. (2019) combined the power spectral density with a convolutional neural network for differentiating MCI, AD, and healthy subjects using EEG signals. The authors reported an accuracy of 83.3% differentiating AD, MCI, and healthy patients, which indicates that further investigations are required in order to identify patterns or features in the EEG signals capable of differentiating AD, MCI, and healthy subjects.

In this work, a new EEG-based methodology is presented for differentiating MCI, AD, and healthy subjects employing the discrete wavelet transform (DWT) (Yuan et al. 2018; Wang et al. 2019; Chang et al. 2019), dispersion entropy index (DEI), a nonlinear measurement proposed recently by Rostaghi and Azami (2016), and a Fuzzy logic-based (FL) classification algorithm (Ma et al. 2018; Javidan and Kim 2019). In this work, it is hypothesized that DEI method would identify patterns or differences among the EEG signals from AD and MCI-patients, and healthy control (HC) subjects, and that these patterns or features could be employed to aid in the classification of different dementia stages (AD vs MCI vs HC). The effectiveness and usefulness of the proposed methodology are evaluated by employing a database of measured EEG data acquired from 135 subjects, 45 MCI, 45 AD and 45 normal subjects.

2. MATERIALS

2.1. Subjects

Three groups of subjects were enrolled within this study at IRCCS Centro Neurolesi Bonino Pulejo (Messina, Italy): 45 AD patients (22 females, mean age 76.13 ± 13.16), 45 amnesic MCI subjects (20 females, mean age 72.55 ± 9.3) and 45 elderly healthy controls (18 females, mean age 72.82 ± 10.12), which can be considered age-matched.

The study was conducted according to a specific protocol approved by the local Ethics Committee of IRCCS Centro Neurolesi (Prot. E29/16). AD patients were under a medical treatment based on cholinesterase inhibitors (ChEis) with a dosage of 20 mg/day. No anti-psychotics or anti-epileptic drugs were administered. Anti-depressants (citalopram) were administered to AD patients in the morning, with a typical dosage of 30 mg/day. The subjects were fully evaluated to assess the possible presence of other psychiatric or neurological conditions such as stroke, tumors, fluids in the brain or other complex systemic disorders. The presence of epileptiform EEG patterns as well as any treatment with any psychoactive medication were also taken into account.

Every participant, or his/her caregiver in case the subject was not cooperative because of dementia, was carefully informed about the objectives and the procedures of the study and signed a consent form.

The experiments were carried out in the morning. The participants remained seated on a comfortable chair and kept his/her eyes closed throughout. **The guidelines of the 5th edition of the diagnostic and statistical manual of mental disorders (APA, 2013) were followed to formulate a diagnosis for each participant of HC, AD or MCI by a team of experts consisting of psychologists, neurologists, psychiatrists, and EEG experts.**

2.2 EEG data

In order to measure the EEG signals of each participant, an EEG headset with 19-channels montage set up according to the 10–20 international system was employed with a linked earlobe (A1–A2) reference. It contains 2 sensors located in the pre-frontal area of brain, Fp1 and Fp2, 5 sensors in the frontal area, F3, F4, F7, F8, and Fz, 4 sensors in the temporal area, T3, T4, T5, and T6, 3 sensors in the parietal area, P3, P4, and Pz, 3 sensors in central area, C3, C4, and Cz, and 2 sensors located in occipital area, O1 and O2.

In order to introduce the least possible distortion, except band pass filtering, EEGs were manually inspected by EEG experts who removed visible blinks and excluded the

artifactual epochs, resulting in EEG signals with an average length of 137.5 ± 102.5 seconds. Hence, to maintain the consistency into the proposed methodology, 35 seconds of artifact-free EEG signal was selected for each patient, yielding 8,960 samples with a sampling frequency of 256 Hz (EEGs were recorded using the Micromed Brain Quick system). A band-pass filter at 0.5-32 Hz was applied to each n-channel EEG recording as this frequency range or bandwidth is perceived to contain the waves related to the brain activities of interest (Ieracitano et al., 2019). Filters were implemented using the open source Matlab's toolbox EEGlab (Delorme & Makeig, S. 2004), specifically, by means of the function `eegfiltfft` which is based on Fast Fourier Transform (FFT) and inverse FFT to reconstruct the signals in the frequency range of interest.

Figure 1 shows examples of the acquired EEG signals at three different places of brain: pre-frontal (Fp1), central (C3), and occipital (O1), for an HC, MCI, and AD subject, respectively. This figure shows that significant differences among the three groups, HC, MCI, and AD, cannot be detected visually. Hence, the main aim of this investigation is to present a new methodology for discovering the differences among the HC, MCI, and AD groups using EEG signals.

3. PROPOSED METHODOLOGY

A macro flowchart of the proposed methodology for discriminating HC, MCI, and AD subjects is presented schematically in Figure 2. It includes four steps. In the first step, the measured EEG signals are decomposed by means of DWT in the four neurophysiological frequency bands: delta (0.5–4 Hz), theta (4–8 Hz), alpha (8–14 Hz), beta (14–30 Hz) (Adeli et al. 2003). In step 2, the frequency bands corresponding to the EEG sub-bands are analyzed by DEI, a nonlinear measurement, for discovering patterns or features capable of differentiating the three groups: HC, MCI and AD. In step 3, the estimated DEI values for each EEG sub-band are evaluated statistically by Kruskal-Wallis method (KWM) in order to determine and select the most discriminant patterns and EEG sub-band(s) for differentiating HC, MCI, and AD subjects. Finally, the patterns or features selected according to KWM method are employed to construct the FL classifier to differentiate the three groups. The steps of the methodology are described in detail in the following sub sections.

3.1 Step 1: Discrete Wavelet Transform

DWT, a time-frequency method, is characterized as an effective tool for analyzing signals with transient, nonlinear and nonstationary properties such as EEG signals (Adeli et al. 2013; Ahmadlou et al. 2011; Ghorbanian et al. 2013; Yuan et al. 2018, Sharma et al. 2020), allowing hidden patterns or features to be revealed in the evaluated signal (Beura et al. 2015). DWT is based on a set of low- and high-pass filters known as approximations (A) and details (D). According to multiresolution analysis, the analyzed signal is decomposed in an approximation (A_1) and a detail (D_1) in the first level, then, A_1 is decomposed in a new approximation and detail and this procedure is repeated, as shown in Figure 3 (Daubechies, 1988).

The frequency range for each approximation and detail according to the analyzed level, L , and sampling frequency, F_s , is given by (Daubechies, 1992):

$$A_L = \left[0, \frac{F_s}{2^{L+1}} \right] \quad (1)$$

$$D_L = \left[\frac{F_s}{2^{L+1}}, \frac{F_s}{2^L} \right] \quad (2)$$

The EEG signals of the three different groups, HC, MCI, and AD, are decomposed up to the fifth level using the DWT. It is important to note that the details of the third-, fourth-, and fifth-level correspond to the frequency ranges beta, alpha, and theta, respectively, and the approximation obtained in the fifth level corresponds with the frequency band delta, which are analyzed in this work.

Different wavelet mother functions (WMFs) such as Daubechies, coiflets, Meyer, among others, have been employed for performing the DWT (Amezquita-Sanchez and Adeli, 2016). Nevertheless, according to Adeli et al. (2003) Daubechies 4 is the most appropriate to analyze EEG signals because it provides a good fit for the patterns or features found in them. For this reason, Daubechies 4 is used as the WFM in this work.

3.2 Step 2: Dispersion Entropy Index (DEI)

DEI is a nonlinear index capable of measuring the irregularity and uncertainties found in a signal (Rostaghi and Azami 2016). In this research, DEI is explored as a measurement

tool for brain dynamic, and is shown to be a suitable index for differentiating the three groups HC, MCI, and AD.

The DEI of a time signal $x_j(j=1, \dots, N)$ with N samples is calculated as follows:

a) Mapping the time signal, X_j , to c classes $u_j(j=1, \dots, N)$ with integer indices from 1 to c .

This step is performed by employing a sigmoid function, also called, normal cumulative distribution function, described in detail in Rostaghi and Azami, (2016).

b) Partition the signal obtained in (a), in a set of new sequences or signals $\mathbf{u}_i^{m,c}$ with an embedding dimension m and a time delay d as:

$$\mathbf{u}_i^{m,c} = \{u_i^c, u_{i+d}^c, \dots, u_{i+(m-1)d}^c\} \text{ for } i = 1, \dots, N - (m-1)d \quad (3)$$

c) Map each new sequence $\mathbf{u}_i^{m,c}$ into a dispersion pattern, $\pi_{v_0 v_1 \dots v_{m-1}}$, as follows:

$$u_i^c = v_0, u_{i+d}^c = v_1, u_{i+(m-1)d}^c = v_{m-1} \quad (4)$$

where each new sequence $\mathbf{u}_i^{m,c}$ has a number of possible dispersion patterns equal to c^m .

d) Calculate a relative frequency for each possible dispersion pattern $\pi_{v_0 v_1 \dots v_{m-1}}$, as:

$$p(\pi_{v_0 v_1 \dots v_{m-1}}) = \frac{\#\{i \mid i \leq N - (m-1)d, \mathbf{u}_i^{m,c} \text{ has type } \pi_{v_0 v_1 \dots v_{m-1}}\}}{N - (m-1)d} \quad (5)$$

e) Compute DEI as follows:

$$DE(x, m, c, d) = -\sum_{\pi=1}^{c^m} p(\pi_{v_0 v_1 \dots v_{m-1}}) \ln p(\pi_{v_0 v_1 \dots v_{m-1}}) \quad (6)$$

Hence, DEI is applied to each decomposed signal or neurophysiological band estimated by DWT in order to estimate patterns or features capable of differentiating the three classes MCI, AD, and HC. Dispersion Entropy Index requires 3 parameters, m (the embedding dimension), c (the number of classes), and d (the time lag), to estimate the irregularity of time series signals. Rostaghi et al. (2019) provided guidelines about the selection of these parameters, such as m should be small when the signal contains few data as analyzed in this work because if m is large, the DEI will be unable to observe small variations in the time series signal. On the other hand, c should be larger than m when the signals contain a small quantity of data in order to be less sensitive to noise contained in the signal. Finally, the authors mention that $d = 1$ is an optimal value. In this sense, the authors

recommend $m = 2$, $c = 6$, and $d = 1$ for analysis of noisy signals with few data and nonstationary properties, such as those analyzed in this work. In addition, these values have been confirmed by other works where different time series signals have been analyzed such as vibration signals, MEG signals, blood pressure signals, and EEG signals [Azami and Escudero 2018; Azami et al. 2019]. Therefore, in this work, these values have been employed, resulting in satisfactory results, where the three groups are classified with good accuracy.

3.3 Step 3: Feature Selection

For evaluating the statistical significance of diverse groups of features estimated by DEI, the KWM test is performed. It is known as an effective statistical tool for comparing patterns or features with non-normal or unknown distributions obtained from different analytical or experimental conditions in order to determinate if they present a significant or insignificant difference among values or sets of values. In particular, the KWM computes a p-value according to a chi-square distribution, which indicates the probability of rejecting a null hypothesis (H_0) where the medians of datasets are evaluated in order to identify if they are equal (Kruskal and Wallis, 1952). If p-value takes a value smaller than a significance level (commonly 0.05) the implication is that the H_0 is rejected, indicating a high capability of features analyzed for differentiating the groups (Bashar et al. 2016). Hence, the p-value estimated by **KWM is employed for determining the most useful DEI values considering the neurophysiological EEG sub bands estimated by DWT and 19 channels in order to help in the distinction of three groups.**

3.4 Step 4: Fuzzy Logic classifier

Finally, the most discriminant DEI values chosen according to the KWM are employed to construct an FL classifier for differentiating HC, MCI and AD automatically. FL is an effective classifier for dealing with overlapped classes as well as for handling uncertainties and vagueness in the datasets (Zadeh, 1965; Abbasi et al. 2019). Because of these advantages, FL classifier has been employed for diagnosis of diabetes (Ganji and Abadeh, 2011), cardiovascular diseases (Sanz et al., 2014), Parkinson's disease (Abiyev and Abizade, 2016), breast cancer (Nilashi et al., 2017), and AD (Kar and Majumder, 2019). Therefore, FL classifier is employed in this work for discriminating among HC, MCI, and

AD patients. For a detailed description of an FL system, the reader should refer to Siddique and Adeli, (2013).

4. VALIDATION OF THE MODEL'S EFFICACY

Following the steps of the proposed method, first the DWT algorithm is used to decompose the EEG signals obtained from 19-channels of the HC, MCI, and AD subjects in their four neurophysiological bands. Then, the DEI method is used for calculating the irregularity value for each of the four EEG sub-bands. Figure 4 (a) to (c) illustrate samples of the four neurophysiological or EEG bands frequency bands obtained after employing DWT method for channels Fp1, C3, and O1 shown in Figure 1 for HC, MCI, and AD subjects, respectively. Significant differences among three groups cannot be determined visually. Therefore, DEI method is used in the next step of the proposed method for discovering hidden patterns in the EEG sub-bands.

Once that the patterns from neurophysiological bands and 19-channels have been obtained by employing the DEI method, they are evaluated by using KWM to mathematical markers with ability to differentiate the three groups. According to the KWM results, the first detail in the range of beta band, from 16 to 32 Hz, of the channels T5 and O2, produced the lowest p-values (10^{-17}), indicating that they can be useful for discriminating the three groups. Table 1 presents the p-values calculated by the KWM for diverse EEG sub-bands and 19 channels for differentiating MCI and AD groups from HC patients. The results confirm that the channels T5 and O2 for the beta band, highlighted on a gray background, present the lowest p-values, which indicate their high capability for differentiating the three classes evaluated in this work.

Figure 5(a) and 5(b) show distribution of the estimated DEI values for the channels T5 and O2, the most discriminant values, respectively. According to this figure, the DEI values calculated for the MCI and AD groups present higher values than those in the HC group, indicating that both MCI and AD groups present an increase in the transient or chaotic characteristics into the EEG signals, which can be associated with the severity of the neurological disorder. Further, the DEI values for three groups present a slight overlap, generating an uncertainty for correct classification of the three groups. Hence, this discovery

lead the authors to use an FL classifier, which can work satisfactorily with overlapping datasets.

Finally, the estimated DEI values for the channels T5 and O2, the most discriminant features, are used to design a FL classifier for differentiating the three groups. **It is important to mention that the 50% of data (22 EEG signals from HC, AD, and MCI patients, respectively) were employed to identify the most discriminant EEG sub-band(s) combined with DEI in order to avoid an overfitting of the membership functions in the FL classifier. On the other hand, the other 50% of dataset (23 EEG signals from HC, AD, and MCI patients, respectively) are used to validate the proposal performance (Abbasi et al. 2019).** It uses a Mamdani-type fuzzy inference system with 2 inputs, 1 output, and 9 rules. The inputs are the DEI values of the channels T5 (DEI-T5) and O2 (DEI-O2), respectively, while the output is the patient condition, HC, MCI, and AD. The inputs are partitioned in 3 Gaussian membership functions, as shown in Figure 6(a) and 6(b), which are labeled as follows: small value (SV), normal value (NV), and high value (HV). The Gaussian membership function is employed because it provides the best alternative according to the input values shown in Figure 5. The Mamdani FL system output assumes values between 0.5 and 3.5 as shown in Figure 6(c), where $HC = 1$, $MCI = 2$, and $AD = 3$. Table 2 summarizes the rules for each regime. For example, one rule can be read as follows: if DEI value of the channel T5 is SV and the DEI value of the channel O2 is SV then the patient condition is HC. The minimum composition and the center-of-gravity method were employed for quantifying the output of the rules and defuzzification, respectively (Passino et al., 1998).

Table 3 summarizes the classification accuracies of the proposed FL classifier for distinguishing the three groups, employing the EEG signals from 135 patients (45 with MCI, 45 with AD and 45 normal patients). HC vs MCI vs AD are identified with an accuracy of 82.6-86.9% This result can be somehow expected due to the existence of overlaps in the DEI values distribution shown in Figure 5, which indicates that, in probabilistic terms, there is not a complete separation among groups. Nevertheless, according to these results, the proposed methodology is an effective tool for differentiating the three groups of MCI, AD, and healthy subjects in an automated manner. On the other hand, if the proposed methodology is used to differentiate two groups, i.e., MCI vs HC, MCI vs AD, and AD vs HC, accuracies of 89%, 91%, and 97% are obtained, respectively. It is important to mention that AD vs HC presents

higher accuracy than other two combinations (MCI vs AD, MCI vs HC), which can be attributed to the large separation of both data distributions shown in Figure 5.

5. COMPARISON WITH PREVIOUS WORKS

Distinguishing among the three classes, HC, MCI, and AD, with good accuracy is a challenging task because the EEG signals are embedded in high-level noise and present a non-stationary and chaotic behavior. The proposed methodology presented reliable results for distinguishing among the three classes studied in this work, HC vs MCI vs AD, reaching an accuracy of 82.6-86.9%. In this regard,

Table 4 presents a qualitative comparison between the proposed methodology and other works introduced in the literature in the past ten years, where the signal processing techniques or methods employed for diagnosing/differentiating MCI and AD patients, as well as their reported accuracy are presented. This table shows the researchers have focused mainly on generating methodologies for differentiating two classes, HC vs MCI, HC vs AD, and MCI vs AD, achieving an accuracy higher than 65% (Ahmadlou et al. 2011 & 2014; Bruña et al. 2012; Houmani et al. 2015; Amezquita-Sanchez et al. 2016; Mammone et al. 2017 & 2018). In the past few years, researchers have presented methodologies for differentiating among the diverse dementia stages, HC vs MCI vs AD, achieving an accuracy higher than 81.8% (Morabito et al. 2016; Houmani et al. 2018; Ieracitano et al. 2019 & 2020). Although these works have obtained promising results, they require diverse nonlinear measurements to identify proper patterns or features in order to determine the various dementia stages, which increases the methodology complexity and their combination do not guarantee to obtain the best possible results.

In contrast, the methodology presented in this paper (DWT, DEI, and FL classifier) offers a reliable tool for distinguishing among the three classes (AD vs MCI vs HC) with the following advantages over the other methods introduced in the literature: (1) it does not require a domain transformation of EEG signals (Ieracitano et al. 2019 & 2020), (2) nor a complicated calibration of the model, and (3) uses only one nonlinear measurement, DEI, to identify reliable patterns or features in the EEG signals, indicating that the new method presents a low complexity computational solution with an accuracy higher than previous

works. Despite these advantages, it is necessary to continue investigating the proposed methodology performance with a larger EEG database, which includes EEG signals measured in diverse stages of illness with a larger range of age, in order to modify or calibrate (e.g., wavelet mother and level decomposition in wavelet transform and the input parameters for DEI method) according to these new circumstances.

6. CONCLUSIONS

EEG signals measured from MCI and AD patients do not present significant visual differences compared with those obtained for health subjects. In this paper, a new methodology was introduced for discriminating patients affected by MCI and AD from HC subjects through adroit integration of the DWT, DEI, a new nonlinear feature, and an FL classifier employing EEG signals. The MCI data present a significant overlap with the HC and AD data. An FL classifier was selected because it can handle overlapping classes as well as uncertainties and vagueness in the datasets effectively (D'Urso et al. 2018; Palacios et al. 2019).

For verifying the accuracy of the proposed methodology, the measured EEG signals from 135 patients (45 with MCI, 45 with AD, and 45 HC) were employed. The proposed method, DWT combined with DEI and an FL classifier, demonstrated to be a useful tool for differentiating MCI and AD patients from HC subjects (HC vs MCI vs AD) with an accuracy of 82.6-86.9%, sensitivity of 91%, and specificity of 87%, **indicating that the proposal can identify significant patterns or features into the measured EEG signals to differentiate among the three groups without import the gender**, which is consistent with previous research (Tom et al. 2015).

The results reported in this investigation must be considered preliminary because of the limited size of the EEG database. The proposed methodology should be further investigated, and its accuracy verified using larger databases. In addition, other alternatives to decompose the EEG signals, such as digital filters, can be investigated in order to reduce the computational complexity.

7. ACKNOWLEDGEMENT

Nadia Mammone's work was funded by the Italian Ministry of Health, project code: GR-2011-02351397. The authors would like to thank Dr. Simona De Salvo (IRCCS Centro Neurolesi Bonino-Pulejo, Italy) for collecting and providing the EEGs.

References

- A.P. Association (Ed.) (2013), *Diagnostic and Statistical Manual of Mental Disorders*, (fifth ed.), Arlington: American Psychiatric Publishing.
- Abbasi, H., Bennet, L., Gunn, A. J., & Unsworth, C. P. (2019). Latent phase detection of hypoxic-ischemic spike transients in the EEG of preterm fetal sheep using reverse biorthogonal wavelets & fuzzy classifier. *International Journal of Neural Systems*, 29(10), 1950013, (17 pages)
- Abiyev, R. H., & Abizade, S. (2016). Diagnosing Parkinson's diseases using fuzzy neural system. *Computational and mathematical methods in medicine*, 2016, 1-12.
- Acharya, U. R., Oh, S. L., Hagiwara, Y., Tan, J. H., & Adeli, H. (2018). Deep convolutional neural network for the automated detection and diagnosis of seizure using EEG signals. *Computers in biology and medicine*, 100, 270-278.
- Adeli, H., Ghosh-Dastidar, S., & Dadmehr, N. (2005a). Alzheimer's disease and models of computation: Imaging, classification, and neural models. *Journal of Alzheimer's Disease*, 7(3), 187-199.
- Adeli, H., Ghosh-Dastidar, S., & Dadmehr, N. (2005b). Alzheimer's disease: models of computation and analysis of EEGs. *Clinical EEG and Neuroscience*, 36(3), 131-140.
- Adeli, H., Zhou, Z., & Dadmehr, N. (2003). Analysis of EEG records in an epileptic patient using wavelet transform. *Journal of neuroscience methods*, 123(1), 69-87.
- Ahmadlou, M., & Adeli, H. (2010). Enhanced probabilistic neural network with local decision circles: A robust classifier. *Integrated Computer-Aided Engineering*, 17(3), 197-210.

- Ahmadlou, M., Adeli, A., Bajo, R., & Adeli, H. (2014). Complexity of functional connectivity networks in mild cognitive impairment subjects during a working memory task. *Clinical Neurophysiology*, 125(4), 694-702.
- Ahmadlou, M., Adeli, H., & Adeli, A. (2011). Fractality and a wavelet-chaos-methodology for EEG-based diagnosis of Alzheimer disease. *Alzheimer Disease & Associated Disorders*, 25(1), 85-92.
- Amezquita-Sanchez, J. P., Adeli, A., & Adeli, H. (2016). A new methodology for automated diagnosis of mild cognitive impairment (MCI) using magnetoencephalography (MEG). *Behavioural Brain Research*, 305, 174-180.
- Amezquita-Sanchez, J. P., Mammone, N., Morabito, F. C., Marino, S., & Adeli, H. (2019). A novel methodology for automated differential diagnosis of mild cognitive impairment and the Alzheimer's disease using EEG signals. *Journal of Neuroscience Methods*, 322, 88-95.
- Ansari, A.H., Cherian, P.J., Caicedo, A., Naulaers, G., De Vos, M., and Van Huffel, S. (2019), Neonatal Seizure Detection Using Deep Convolutional Neural Networks, *International Journal of Neural Systems*, 29:4, 1850011 (20 pages).
- Azami, H., & Escudero, J. (2018). Amplitude-and fluctuation-based dispersion entropy. *Entropy*, 20(3), 210.
- Azami, H., Fernández, A., & Escudero, J. (2019). Multivariate multiscale dispersion entropy of biomedical times series. *Entropy*, 21(9), 913.
- Bashar, S. K., & Bhuiyan, M. I. H. (2016). Classification of motor imagery movements using multivariate empirical mode decomposition and short time Fourier transform based hybrid method. *Engineering science and technology, an international journal*, 19(3), 1457-1464.
- Beura, S., Majhi, B., & Dash, R. (2015). Mammogram classification using two dimensional discrete wavelet transform and gray-level co-occurrence matrix for detection of breast cancer. *Neurocomputing*, 154, 1-14.

- Bhat, S., Acharya, U. R., Dadmehr, N., & Adeli, H. (2015). Clinical neurophysiological and automated EEG-based diagnosis of the Alzheimer's disease. *European neurology*, 74(3-4), 202-210.
- Blennow, K. Leon MJ de, Zetterberg H (2006) Alzheimer's disease. *Lancet*, 368, 387-403.
- Bruña, R., Poza, J., Gómez, C., García, M., Fernández, A., & Hornero, R. (2012). Analysis of spontaneous MEG activity in mild cognitive impairment and Alzheimer's disease using spectral entropies and statistical complexity measures. *Journal of Neural Engineering*, 9(3), 036007.
- Cai, Q., Gao, Z. K., Yang, Y. X., Dang, W. D., & Grebogi, C. (2019). Multiplex limited penetrable horizontal visibility graph from EEG signals for driver fatigue detection. *International Journal of Neural Systems*, 29(5), 1850057 (10 pages)
- Chang, Z., De Luca, F., & Goda, K. (2019). Automated classification of near-fault acceleration pulses using wavelet packets. *Computer-Aided Civil and Infrastructure Engineering*, 34(7), 569-585.
- Collazos-Huertas, D., Cárdenas-Peña, D., & Castellanos-Dominguez, G. (2019). Instance-based representation using multiple kernel learning for predicting conversion to Alzheimer disease. *International Journal of Neural Systems*, 29(02), 1850042 (12 pages).
- Corsi, M. C., Chavez, M., Schwartz, D., Hugueville, L., Khambhati, A. N., Bassett, D. S., & de Vico Fallani, F. (2019). Integrating EEG and MEG signals to improve motor imagery classification in brain-computer interface. *International Journal of Neural Systems*, 29(01), 1850014 (12 pages).
- Daubechies, I. (1988). Orthonormal bases of compactly supported wavelets. *Communications on pure and applied mathematics*, 41(7), 909-996.
- Daubechies, I. (1992). *Ten lectures on wavelets*. Philadelphia, PA: Soc. Ind. Appl. Math., 61, 1-340.
- delEtoile, J., & Adeli, H. (2017). Graph theory and brain connectivity in Alzheimer's disease. *The Neuroscientist*, 23(6), 616-626.

- Delorme, A., & Makeig, S. (2004). EEGLAB: an open source toolbox for analysis of single-trial EEG dynamics including independent component analysis. *Journal of neuroscience methods*, 134(1), 9-21.
- D'Urso, M. G., Masi, D., Zuccaro, G., & De Gregorio, D. (2018). Multicriteria fuzzy analysis for a GIS-based management of earthquake scenarios. *Computer-Aided Civil and Infrastructure Engineering*, 33(2), 165-179.
- Fang, C., Li, C., Cabrerizo, M., Barreto, A., Andrian, J., Rishe, N., Loewenstein, D., Duara, R., & Adjouadi, M. (2018), Gaussian discriminant analysis-based dual high-dimensional decision spaces for the diagnosis of mild cognitive impairment in Alzheimer's disease. *International Journal of Neural Systems*, 28(8).
- Gálvez, G., Recuero, M., Canuet, L., & Del-Pozo, F. (2018). Short-Term Effects of Binaural Beats on EEG Power, Functional Connectivity, Cognition, Gait and Anxiety in Parkinson's Disease. *International journal of neural systems*, 28(05), 1750055.
- Ganji, M. F., & Abadeh, M. S. (2011). A fuzzy classification system based on Ant Colony Optimization for diabetes disease diagnosis. *Expert Systems with Applications*, 38(12), 14650-14659.
- Gauthier, S., Reisberg, B., Zaudig, M., Petersen, R. C., Ritchie, K., Broich, K., & Cummings, J. L. (2006). Mild cognitive impairment. *The lancet*, 367(9518), 1262-1270.
- Ghorbanian, P., Devilbiss, D. M., Verma, A., Bernstein, A., Hess, T., Simon, A. J., & Ashrafiun, H. (2013). Identification of resting and active state EEG features of Alzheimer's disease using discrete wavelet transform. *Annals of biomedical engineering*, 41(6), 1243-1257.
- Houmani, N., Dreyfus, G., & Vialatte, F. B. (2015). Epoch-based Entropy for Early Screening of Alzheimer's Disease. *International Journal of Neural Systems*, 25(08), 1550032.
- Houmani, N., Vialatte, F., Gallego-Jutglà, E., Dreyfus, G., Nguyen-Michel, V. H., Mariani, J., & Kinugawa, K. (2018). Diagnosis of Alzheimer's disease with Electroencephalography in a differential framework. *PloS one*, 13(3), e0193607.

- Hulbert, S., & Adeli, H. (2013). EEG/MEG-and imaging-based diagnosis of Alzheimer's disease. *Reviews in the neurosciences*, 24(6), 563-576.
- Ibáñez-Molina, A. J., Iglesias-Parro, S., & Escudero, J. (2019). Differential effects of simulated cortical network lesions on synchrony and EEG complexity. *International Journal of Neural Systems*, 29(04), 1850024 (17 pages)
- Ibrahim, S., Djemal, R., & Alsuwailem, A. (2018). Electroencephalography (EEG) signal processing for epilepsy and autism spectrum disorder diagnosis. *Biocybernetics and Biomedical Engineering*, 38(1), 16-26.
- Ieracitano, C., Mammone, N., Bramanti, A., Hussain, A., & Morabito, F. C. (2019). A Convolutional Neural Network approach for classification of dementia stages based on 2D-spectral representation of EEG recordings. *Neurocomputing*, 323, 96-107.
- Ieracitano, C., Mammone, N., Hussain, A., & Morabito, F. C. (2020). A novel multi-modal machine learning based approach for automatic classification of EEG recordings in dementia. *Neural Networks*, 123, 176-190.
- Javidan, M. M., & Kim, J. (2019). Variance-based global sensitivity analysis for fuzzy random structural systems. *Computer-Aided Civil and Infrastructure Engineering*, 34(7), 602-615.
- Kar, S., & Majumder, D. D. (2019). A Novel Approach of Diffusion Tensor Visualization Based Neuro Fuzzy Classification System for Early Detection of Alzheimer's Disease. *Journal of Alzheimer's disease reports*, 3(1), 1-18.
- Kruskal, W. H., & Wallis, W. A. (1952). Use of ranks in one-criterion variance analysis. *Journal of the American statistical Association*, 47(260), 583-621.
- Kutner, M. H., Nachtsheim, C. J., Neter, J., & Li, W. (2005). *Applied linear statistical models* (Vol. 5). New York: McGraw-Hill Irwin.
- Lauttia, J., Helminen, T. M., Leppänen, J. M., Yrttiaho, S., Eriksson, K., Hietanen, J. K., & Kylliäinen, A. (2019). Atypical Pattern of Frontal EEG Asymmetry for Direct Gaze in Young Children with Autism Spectrum Disorder. *Journal of Autism and Developmental Disorders*, 49(9), 3592-3601.

- Ma, L., Sacks, R., Kattel, U., & Bloch, T. (2018). 3D object classification using geometric features and pairwise relationships. *Computer-Aided Civil and Infrastructure Engineering*, 33(2), 152-164.
- Mammone, N., Bonanno, L., Salvo, S. D., Marino, S., Bramanti, P., Bramanti, A., & Morabito, F. C. (2017). Permutation disalignment index as an indirect, EEG-based, measure of brain connectivity in MCI and AD patients. *International Journal of Neural Systems*, 27(05), 1750020.
- Mammone, N., Ieracitano, C., Adeli, H., Bramanti, A., & Morabito, F. C. (2018). Permutation jaccard distance-based hierarchical clustering to estimate EEG network density modifications in MCI subjects. *IEEE Transactions on Neural Networks and Learning Systems*, 29(10), 5122-5135.
- Martínez-Rodrigo, A., García-Martínez, B., Alcaraz, R., González, P., & Fernández-Caballero, A. (2019). Multiscale entropy analysis for recognition of visually elicited negative stress from EEG recordings. *International Journal of Neural Systems*, 29(02), 1850038 (17 pages).
- Martínez-Vargas, J. D., Duque-Muñoz, L., Vargas-Bonilla, F., López, J. D., & Castellanos-Dominguez, G. (2019). Enhanced Data Covariance Estimation Using Weighted Combination of Multiple Gaussian Kernels for Improved M/EEG Source Localization. *International Journal of Neural Systems*, 29(06), 1950001 (15 pages)
- Mirzaei, G., Adeli, A., & Adeli, H. (2016). Imaging and machine learning techniques for diagnosis of Alzheimer's disease. *Reviews in the Neurosciences*, 27(8), 857-870.
- Mitchell, A. J., & Shiri-Feshki, M. (2009). Rate of progression of mild cognitive impairment to dementia—meta-analysis of 41 robust inception cohort studies. *Acta Psychiatrica Scandinavica*, 119(4), 252-265.
- Morabito, F. C., Campolo, M., Ieracitano, C., Ebadi, J. M., Bonanno, L., Bramanti, A. & Bramanti, P. (2016). Deep convolutional neural networks for classification of mild cognitive impaired and Alzheimer's disease patients from scalp EEG recordings. *IEEE, 2nd International Forum in Research and Technologies for Society and Industry Leveraging a better tomorrow (RTSI)*, Bologna, Italy, pp. 1-6.

- Mumtaz, W., Ali, S. S. A., Yasin, M. A. M., & Malik, A. S. (2018). A machine learning framework involving EEG-based functional connectivity to diagnose major depressive disorder (MDD). *Medical & biological engineering & computing*, 56(2), 233-246.
- Nilashi, M., Ibrahim, O., Ahmadi, H., & Shahmoradi, L. (2017). A knowledge-based system for breast cancer classification using fuzzy logic method. *Telematics and Informatics*, 34(4), 133-144.
- Nobukawa, S., Yamanishi, T., Nishimura, H., Wada, Y., Kikuchi, M., & Takahashi, T. (2019). Atypical temporal-scale-specific fractal changes in Alzheimer's disease EEG and their relevance to cognitive decline. *Cognitive neurodynamics*, 13(1), 1-11.
- Palacios, J.J., González-Rodríguez, I., Vela, C.R., and Puente, J. (2019), Satisfying flexible due dates in fuzzy job shop by means of hybrid evolutionary algorithms, *Integrated Computer-Aided Engineering*, 26:1, pp. 65-84.
- Passino, K.M., Yurkovich, S., & Reinfrank, M. *Fuzzy Control*; Addison-Wesley: Menlo Park, CA, USA, 1998.
- Petersen, R. C., Doody, R., Kurz, A., Mohs, R. C., Morris, J. C., Rabins, P. V., & Winblad, B. (2001). Current concepts in mild cognitive impairment. *Archives of neurology*, 58(12), 1985-1992.
- Rostaghi, M., & Azami, H. (2016). Dispersion entropy: A measure for time-series analysis. *IEEE Signal Processing Letters*, 23(5), 610-614.
- Rostaghi, M., Ashory, M. R., & Azami, H. (2019). Application of dispersion entropy to status characterization of rotary machines. *Journal of Sound and Vibration*, 438, 291-308.
- Sanz, J. A., Galar, M., Jurio, A., Brugos, A., Pagola, M., & Bustince, H. (2014). Medical diagnosis of cardiovascular diseases using an interval-valued fuzzy rule-based classification system. *Applied Soft Computing*, 20, 103-111.
- Schetinin, V., Jakaite, L., Nyah, N., Novakovic, D., & Krzanowski, W. (2018). Feature extraction with GMDH-type neural networks for EEG-based person identification. *International Journal of Neural Systems*, 28(06), 1750064 (23 pages).

- Shanir, P. M., Khan, K. A., Khan, Y. U., Farooq, O., & Adeli, H. (2017). Automatic Seizure Detection Based on Morphological Features Using One-Dimensional Local Binary Pattern on Long-Term EEG. *Clinical EEG and neuroscience*, 1550059417744890.
- Sharma, M., Patel, S., & Acharya, U. R. (2020). Automated detection of abnormal EEG signals using localized wavelet filter banks. *Pattern Recognition Letters*, 133, 188-194.
- Siddique, N., & Adeli, H. (2013). *Computational intelligence: synergies of fuzzy logic, neural networks and evolutionary computing*. John Wiley & Sons.
- Simons, S., Espino, P., & Abásolo, D. (2018). Fuzzy entropy analysis of the electroencephalogram in patients with Alzheimer's disease: is the method superior to sample entropy?. *Entropy*, 20(1), 21.
- Sun, C., Cui, H., Zhou, W., Nie, W., Wang, X., & Yuan, Q. (2019). Epileptic Seizure Detection with EEG Textural Features and Imbalanced Classification Based on EasyEnsemble Learning. *International Journal of Neural Systems*, 29(10), 1950021. (17 pages)
- Timothy, L. T., Krishna, B. M., & Nair, U. (2017). Classification of mild cognitive impairment EEG using combined recurrence and cross recurrence quantification analysis. *International Journal of Psychophysiology*, 120, 86-95.
- Trambaiolli, L. R., Lorena, A. C., Fraga, F. J., Kanda, P. A., Anghinah, R., & Nitrini, R. (2011). Improving Alzheimer's disease diagnosis with machine learning techniques. *Clinical EEG and neuroscience*, 42(3), 160-165.
- Triggiani, A. I., Bevilacqua, V., Brunetti, A., Lizio, R., Tattoli, G., Cassano, F., & Babiloni, C (2017). Classification of healthy subjects and Alzheimer's disease patients with dementia from cortical sources of resting state EEG rhythms: a study using artificial neural networks. *Frontiers in neuroscience*, 10, 604.
- Valenzuela, O., Jiang, X., Carrillo, A., & Rojas, I. (2018). Multi-objective genetic algorithms to find most relevant volumes of the brain related to alzheimer's disease and mild

- cognitive impairment. *International Journal of Neural Systems*, 28(09), 1850022 (23 pages)
- Vuksanović, V., Staff, R. T., Ahearn, T., Murray, A. D., & Wischik, C. M. (2019). Cortical thickness and surface area networks in healthy aging, Alzheimer's disease and behavioral variant fronto-temporal dementia. *International journal of neural systems*, 29(06), 1850055 (26 pages).
- Wang, S. H., Zhang, Y. D., Yang, M., Liu, B., Ramirez, J., & Gorriz, J. M. (2019). Unilateral sensorineural hearing loss identification based on double-density dual-tree complex wavelet transform and multinomial logistic regression. *Integrated Computer-Aided Engineering*, 26(4), 411-426.
- Yuan, Q., Zhou, W., Xu, F., Leng, Y., & Wei, D. (2018). Epileptic EEG identification via LBP operators on wavelet coefficients. *International Journal of Neural Systems*, 28(8), 1850010 (16 pages).
- Zadeh, L. A. (1965). Fuzzy sets. *Information and Control*, 8, 338–353.
- Zhang, J., Xiao, M., Gao, L., Chu, S. (2019), "Probability and interval hybrid reliability analysis based on adaptive local approximation of projection outlines using support vector machine," *Computer-Aided Civil and Infrastructure Engineering*, 34:11, 991-1009.
- Zhang, Y., Yao, D., and Xu, P. (2019), "The Dynamic Brain Networks of Motor Imagery: Time-Varying Causality Analysis of Scalp EEG," *International Journal of Neural Systems*, 29:1, 1850016 (16 pages).
- Zieleniewska, M., Duszyk, A., Różański, P., Pietrzak, M., Bogotko, M., & Durka, P. (2019). Parametric description of EEG profiles for assessment of sleep architecture in disorders of consciousness. *International Journal of Neural Systems*, 29(03), 1850049 (17 pages).

Table 1. Estimated p-values by KWM for different EEG sub-bands and channels

| Band | Channel | p-value | Band | Channel | p-value |
|-------------|------------------------|-----------------------|----------------------|----------------|----------------------|
| Beta | Fp1 | 1.3×10^{-2} | Theta | Fp1 | 1.8×10^{-7} |
| | Fp2 | 8.5×10^{-5} | | Fp2 | 1.9×10^{-7} |
| | F7 | 2.3×10^{-8} | | F7 | 3.5×10^{-5} |
| | F3 | 3.5×10^{-5} | | F3 | 1.4×10^{-5} |
| | Fz | 8.4×10^{-5} | | Fz | 1.8×10^{-5} |
| | F4 | 1.0×10^{-2} | | F4 | 3.3×10^{-8} |
| | F8 | 4.4×10^{-8} | | F8 | 1.3×10^{-5} |
| | T3 | 1.3×10^{-8} | | T3 | 1.0×10^{-2} |
| | C3 | 7.8×10^{-5} | | C3 | 1.3×10^{-2} |
| | Cz | 4.1×10^{-5} | | Cz | 7.3×10^{-8} |
| | C4 | 1.3×10^{-5} | | C4 | 5.5×10^{-5} |
| | T4 | 1.6×10^{-5} | | T4 | 3.2×10^{-5} |
| | T5 | 4.8×10^{-17} | | T5 | 1.3×10^{-2} |
| | P3 | 9.0×10^{-11} | | P3 | 1.9×10^{-2} |
| | Pz | 4.0×10^{-11} | | Pz | 5.0×10^{-5} |
| | P4 | 2.0×10^{-11} | | P4 | 7.7×10^{-5} |
| | T6 | 3.6×10^{-14} | | T6 | 7.9×10^{-5} |
| O1 | 5.2×10^{-17} | O1 | 6.1×10^{-5} | | |
| O2 | 1.54×10^{-17} | O2 | 8.7×10^{-5} | | |
| Alpha | Fp1 | 5.3×10^{-8} | Delta | Fp1 | 1.5×10^{-1} |
| | Fp2 | 6.6×10^{-5} | | Fp2 | 4.3×10^{-2} |
| | F7 | 7.5×10^{-5} | | F7 | 7.6×10^{-2} |
| | F3 | 4.4×10^{-8} | | F3 | 2.6×10^{-2} |
| | Fz | 1.1×10^{-5} | | Fz | 1.0×10^{-2} |
| | F4 | 4.4×10^{-5} | | F4 | 8.3×10^{-4} |
| | F8 | 8.7×10^{-5} | | F8 | 1.6×10^{-3} |
| | T3 | 6.3×10^{-5} | | T3 | 2.5×10^{-4} |
| | C3 | 8.9×10^{-5} | | C3 | 6.3×10^{-4} |
| | Cz | 1.6×10^{-2} | | Cz | 2.7×10^{-1} |
| | C4 | 1.8×10^{-2} | | C4 | 3.2×10^{-2} |
| | T4 | 2.1×10^{-2} | | T4 | 9.0×10^{-4} |
| | T5 | 4.9×10^{-2} | | T5 | 3.0×10^{-2} |
| | P3 | 1.6×10^{-2} | | P3 | 2.0×10^{-2} |
| | Pz | 9.0×10^{-5} | | Pz | 1.0×10^{-2} |
| | P4 | 1.9×10^{-2} | | P4 | 4.9×10^{-2} |
| | T6 | 1.7×10^{-2} | | T6 | 2.4×10^{-2} |
| O1 | 2.2×10^{-2} | O1 | 4.4×10^{-2} | | |
| O2 | 6.2×10^{-5} | O2 | 4.7×10^{-2} | | |

Table 2. Rules for the proposed FL classification system.

| Inputs | DEI values for channel T5 | | |
|----------------------------------|----------------------------------|-----|-----|
| DEI values for channel O2 | SV | NV | HV |
| SV | HC | HC | MCI |
| NV | MCI | MCI | AD |
| HV | MCI | AD | AD |

Table 3. Classification results (confusion matrix).

| Patient condition | HC | MCI | AD | Accuracy (%) |
|--------------------------|-----------|------------|-----------|---------------------|
| HC | 21 | 2 | 0 | 91.3 |
| MCI | 3 | 19 | 1 | 82.6 |
| AD | 1 | 2 | 20 | 86.9 |

Table 4. Qualitative comparison between the proposed methodology and other works presented in literature reporting HC, MCI and AD classification.

| Work | Employed methods | Distinction | No. Participants | Accuracy (%) |
|---------------------------------|---|-----------------|-----------------------------|--------------|
| Ahmadlou et al. (2011) | 1. Wavelet transform is used to obtain the EEG sub-bands 2. Feature extraction is performed by using fractal dimension 3. Linear discriminant method is used as classifier. | AD vs HC | HC: 7 AD: 20 | 99.3 |
| Bruña et al. (2012) | 1. Short time Fourier transform is used to identify relevant frequency components related to MCI. 2. Feature extraction is performed by using Euclidean distance, entropies, and statistical complexities. 3. Linear discriminant method is used as classifier. | MCI vs HC | HC: 18 MCI: 26 | 65 |
| Ahmadlou et al. (2014) | 1. Digital filter is used to obtain the EEG sub-bands. 2. Feature extraction is performed by using complexity. 3. EPNN is used as classifier. | MCI vs HC | HC: 19 MCI: 18 | 97.6 |
| Houmani et al. (2015) | 1. Feature extraction is performed by using entropies. 2. Linear discriminant method is used as classifier. | AD vs HC | HC: 32 AD: 30 | 83 |
| Amezquita-Sanchez et al. (2016) | 1. Complete ensemble empirical mode decomposition is used to obtain the EEG sub-bands. 2. Feature extraction is performed by using permutation entropy. 3. EPNN is used as classifier. | MCI vs HC | HC: 19 MCI: 18 | 98.4 |
| Mammone et al. (2017) | 1. Fourier transform is used to obtain the EEG sub-bands. 2. Feature extraction is performed by using permutation disalignment. | AD vs MCI | MCI: 8 AD: 7 | NR |
| Mammone et al. (2018) | 1. Fourier transform is used to obtain the EEG sub-bands. 2. Feature extraction is performed by using permutation Jaccard distance. | AD vs MCI | MCI: 25 AD: 4 | NR |
| Amezquita-Sanchez et al. (2019) | 1. Multiple signal classification and empirical wavelet transform are used to obtain the EEG sub-bands. 2. Feature extraction is performed by using fractal dimension and Hurts exponent for feature extraction. 3. EPNN is used as classifier. | AD vs MCI | MCI: 37 AD: 37 | 90.3 |
| Morabito et al. (2016) | 1. Continuous wavelet transform is used to identify frequency components associated with dementia stages. 2. Convolutional neural network is used as feature extractor and classifier. | AD vs MCI vs HC | HC: 23 MCI: 56 AD: 63 | 78 |

| | | | | |
|--------------------------|---|--------------------|-----------------------------|-----------|
| Houmani et al. (2018) | 1. Feature extraction is performed by using epoch-based entropy and bump modeling. 2. SVM is used as classifier. | AD vs MCI vs HC | HC: 22 MCI: 58 AD: 49 | 81.8 |
| Ieracitano et al. (2019) | 1. Power spectral density is used to identify frequency components associated with dementia stages. 2. Convolutional neural network is used as feature extractor and classifier. | AD vs MCI vs HC | HC: 63 MCI: 63 AD: 63 | 83.3 |
| Ieracitano et al. (2020) | 1. Continuous wavelet transform and bispectrum are used to identify frequency components associated with dementia stages. 2. Feature extraction is performed by using 11 methods. 3. Multilayer neural network is used as classifier. | AD vs MCI vs HC | HC: 63 MCI: 63 AD: 63 | 88.5 |
| This work | 1. Discrete wavelet transform is used to obtain the EEG sub-bands. 2. Feature extraction is performed by using DEI method. 3. FL is used as classifier. | AD vs MCI vs HC | HC: 45 MCI: 45 AD: 45 | 82.6-86.9 |

NR: Not reported.

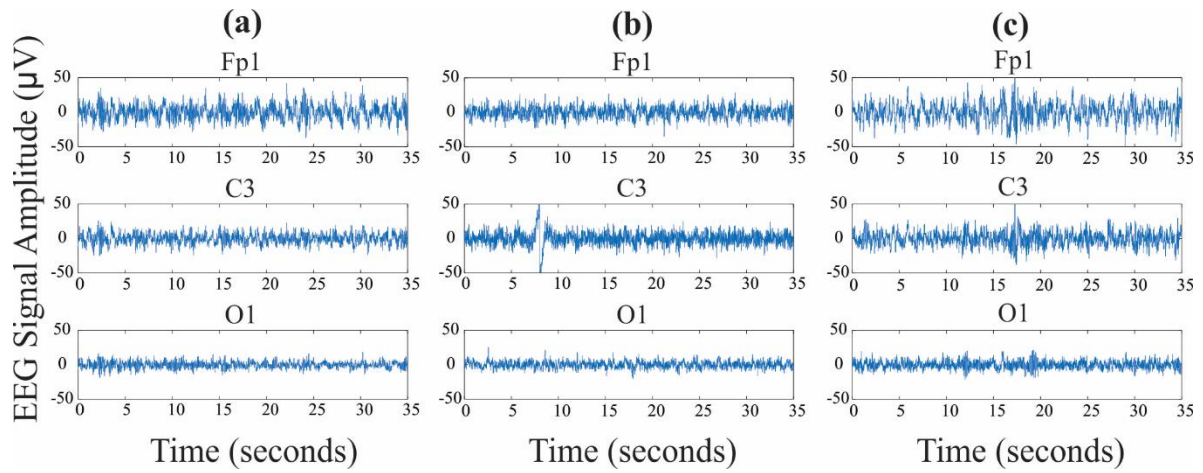


Figure 1 Sample EEG signals acquired at three different locations: pre-frontal (Fp1), central (C3), and occipital lobes (O1) for (a) a HC, (b) an MCI, and (b) an AD subject

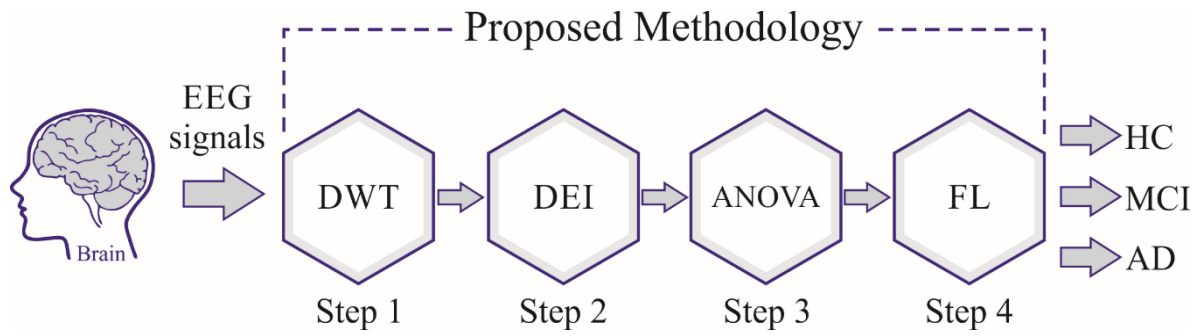


Figure 2. Schematic diagram of the proposed methodology

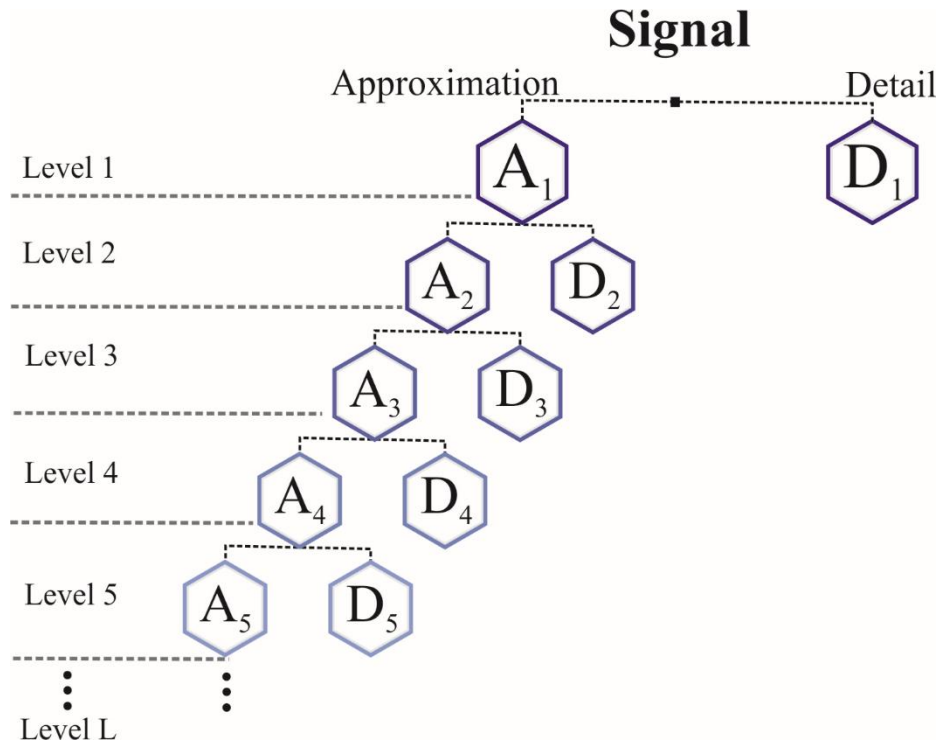


Figure 3. DWT multiresolution analysis

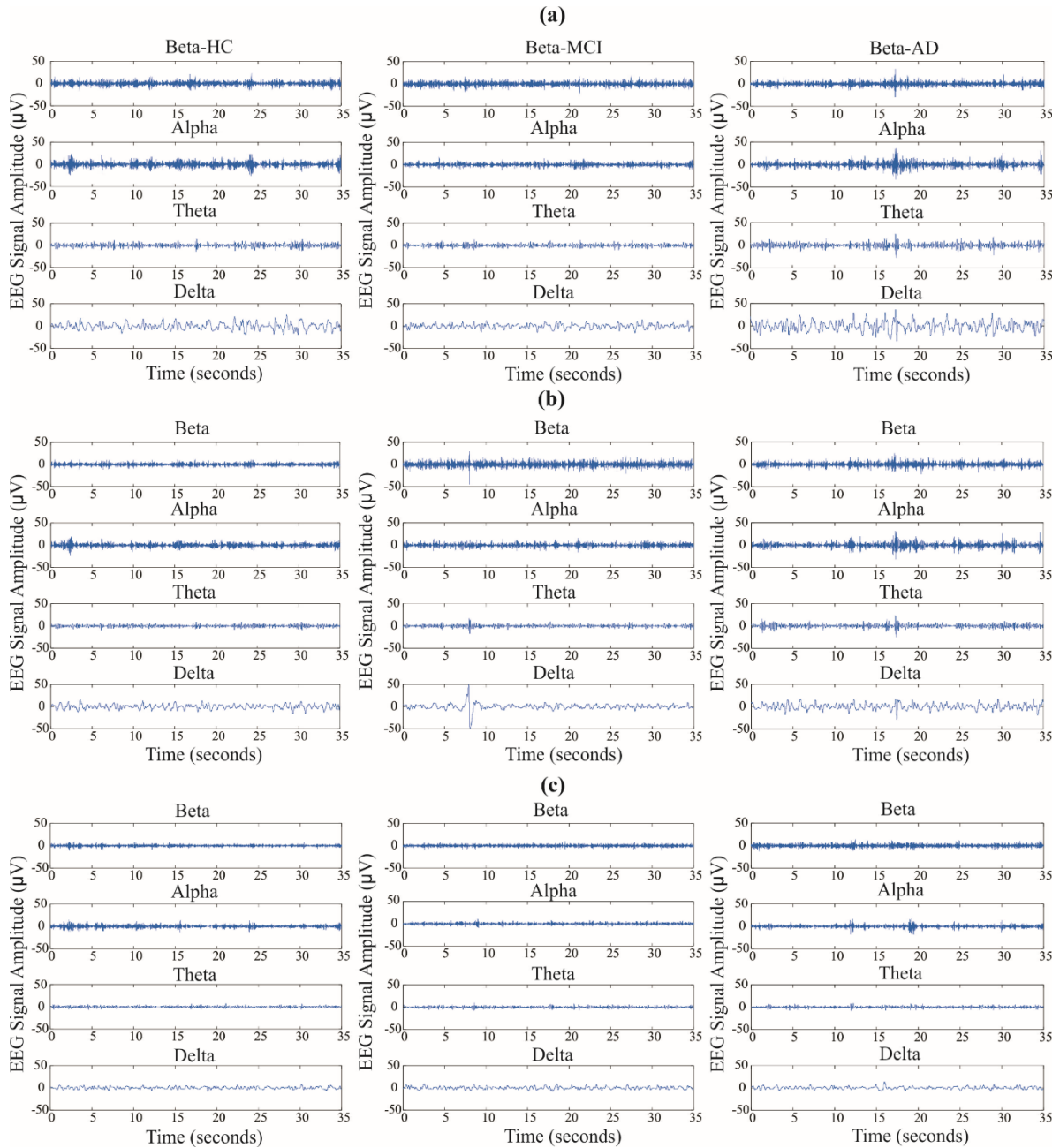


Figure 4. EEG sub-bands obtained after employing DWT algorithm for HC, MCI, and AD patient and channels (a) Fp1, (b) C3, and (c) O1.

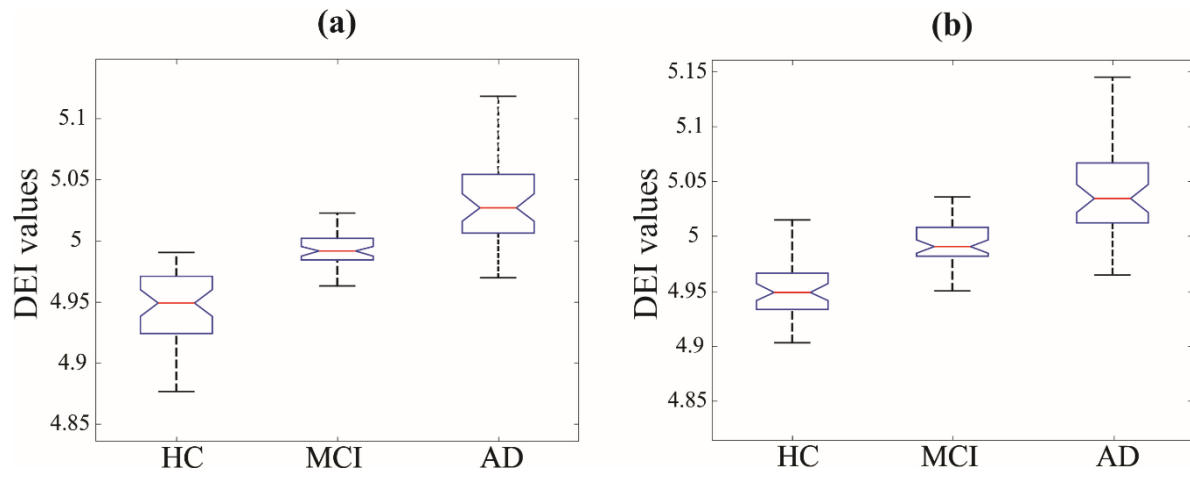


Figure 5. Distribution of the estimated DEI values for HC, MCI, and AD subjects for channels (a) T5 and (b) O2

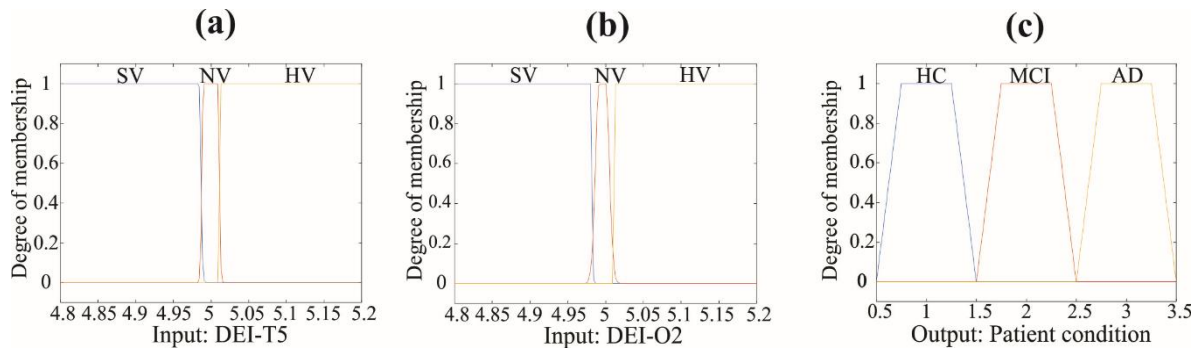


Figure 6. Membership functions for (a) DEI-T5, (b) DEI-O2, and (c) FL output